jet INTL JOURNAL OF ELECTRONICS AND TELECOMMUNICATIONS, 2011, VOL. 57, NO. 3, PP. 347–358
Manuscript received June 27, 2011; revised August 2011. DOI: 10.2478/v10177-011-0047-2

Computationally-Efficient Design of a Dynamic System-Level LTE Simulator

Pablo Muñoz, Isabel de la Bandera, Fernando Ruiz, Salvador Luna-Ramírez, Raquel Barco, Matías Toril, Pedro Lázaro, and Jaime Rodríguez

***Abstract*—The Long-Term Evolution (LTE) is the next generation of current mobile telecommunication networks. LTE has a new flat radio-network architecture and a significant increase in spectrum efficiency. In this paper, a computationally-efficient tool for dynamic system-level LTE simulations is proposed. A physical layer abstraction is performed to predict link-layer performance with a low computational cost. At link layer, there are two important functions designed to increase the network capacity: Link Adaptation and Dynamic Scheduling. Other Radio Resource Management functionalities such as Admission Control and Mobility Management are performed at network layer. The simulator is conceived for large simulated network time to allow evaluation of optimization algorithms for the main network-level functionalities.**

***Keywords*—LTE, simulator, RRM, network, link-level, system-level, E-UTRAN.**

I. Introduction

LTE is the evolution of the current UMTS mobile communication network. This 3GPP standard is the combination of the all-IP core network known as the evolved packet core (EPC) and the evolved UMTS terrestrial radio access network (E-UTRAN). The key benefits of LTE can be summarized in improved system performance, higher data rates and spectral efficiency, reduced latency and power consumption, enhanced flexibility of spectral usage and simplified network architecture.

In LTE, the multiple access scheme is Orthogonal Frequency-Division Multiplexing (OFDM) in the downlink and Single Carrier Frequency Division Multiple Access (SC-FDMA) in the uplink [1]. These techniques achieve a reduction in the interference, thus increasing network capacity. A Physical Resource Block (PRB), which has a bandwidth resolution of 180 kHz, is the minimum amount of frequency resources that can be scheduled for transmission. LTE performs channel-dependent scheduling in both time and frequency, with a resolution of one subframe (1ms) and one PRB, respectively. The scheduler is a fundamental part of the base station due to its influence over system performance.

The access network E-UTRAN [2] is composed basically of just one type of node: the base station called evolved NodeB (eNB). To reduce network elements, all functions that were included in the Radio Network Controller (RNC) in UMTS are located in the eNB in LTE (e.g., radio protocols, mobility management, header compression and security algorithms). The eNBs are connected by standardized interfaces, called X2, which allow multivendor interoperability. In addition, information such as traffic load can be exchanged between eNBs over the X2 interface.

LTE defines a set of advanced functions for Radio Resource Management (RRM) in order to achieve an efficient use of the available resources. These functions include radio bearer control, radio admission control, radio mobility control, scheduling and dynamic allocation of resources. At layer 2, Link Adaptation and Dynamic Packet Scheduling are key features to ensure high spectral efficiency [3] based on user connection quality. On the one hand, Link Adaptation dynamically adjusts the data rate (modulation scheme and channel coding rate) to match the radio channel capacity for each user. The Channel Quality Indicator (CQI) transmitted by the UE, which is an indication of the data rate that can be supported by the channel, is an important input for link adaptation algorithms. On the other hand, Dynamic Scheduling distributes the PRBs among the UEs and the radio bearers of each UE every Transmission Time Interval (TTI) of 1 ms.

At RRM layer 3 [4], Admission Control and Mobility Management are crucial to ensure seamless service as the user moves. Admission Control decides whether the requests for new bearers are granted or rejected, taking into account the available resources in the cell, the QoS requirements for the bearer, the priority levels and the provided QoS to the active sessions in the cell. Mobility management includes procedures for idle and connected UEs. For both types of procedures, the UE periodically performs not only serving cell quality measurements, but also neighboring cell measurements. In idle mode, cell selection selects a suitable cell to camp based on radio measurements. In connected mode, handover decides whether the UE should move to another serving cell. The main difference between UMTS and LTE is that in LTE only hard handovers are defined.

This paper describes the design of a dynamic system-level LTE simulator conceived for large simulated network time. A physical layer abstraction is performed to predict link-layer performance with a low computational cost. Thus, realistic OFDM (Orthogonal Frequency Division Multiplexing) channel realizations with multi-path fading propagation conditions have been generated to obtain an accurate value of Signal-to-Interference Ratio (SIR) for each subcarrier. Then, a method is used to aggregate SIR measurements of several OFDM subcarriers into a single scalar value. Subsequently, Block Error Rate (BLER) is estimated from those SIR values, which is used

This work has partially been supported by the Junta de Andalucía (Excellence Research Program, project TIC-4052) and by the Spanish Ministry of Science and Innovation (grant TEC2009-13413).

All authors are with University of Málaga, Communications Engineering Dept., Campus de Teatinos. 29071, Málaga, Spain (e-mails: {pabloml, ibanderac, ferv, sluna, rbm, mtoril, plazaro}@ic.uma.es, jaime-r-m@alu.uma.es).

in the Link Adaptation and Dynamic Scheduling functions. Additionally, functions for admission control and mobility management are included in the simulator. For computational efficiency, the tool is focused on the downlink of E-UTRAN.

The design of efficient simulation tools for LTE networks has been addressed in the literature. In [5], a simple physical layer model is proposed for LTE in order to reduce the complexity of system level analysis. In [6], a link-level simulator for LTE downlink is presented as an appropriate interface to a system level simulator. In [7], an LTE downlink system-level simulator is proposed for free under an academic, non-commercial use license. The physical layer model is described in [8]. The main purpose of the MATLAB-based simulation tool presented in [7] is to assess network performance of new scheduling algorithms.

This paper proposes the design of a system-level LTE simulator that can be used to evaluate optimization algorithms for the main network-level functionalities, namely handover, admission control and cell reselection. For this purpose, simulations are composed of epochs or optimization loops, where the modification of network parameters can be evaluated. Each epoch is composed of a configurable number of iterations, whose duration is determined by the simulator time resolution. In addition, the size of the simulation scenario must be larger than that in most of the existing LTE simulators, which usually consider only a few cells in the network layout.

This work is organized as follows. Section II presents the general simulator structure. Section III describes the Physical Layer, focusing on the calculation of the OFDM channel realizations needed for resource planning. Section IV is devoted to the Link Layer, where link adaptation and resource planning are performed. Section V outlines the Network Layer, including admission control, congestion control and mobility management. In Section VI, simulation results are presented. Finally, in Section VII, the main conclusions are highlighted.

II. Simulator General Structure

This section presents the general structure of the LTE simulator developed in MATLAB. Fig. 1 shows the main functional blocks of the simulator.

The first stage of a simulation is the initialization of the main simulation parameters, defining the behavior of the main functions in the simulator. The scenario to be simulated is generated here. A warm-up distribution of users is also created by this function, which allows to obtain meaningful network statistics from the first iterations of the simulation.

The next function calculates the propagation losses. This function calculates the power received by each user from the base stations of the scenario. The simulator includes a propagation loss model, a slow fading model and a fast fading model. During this phase, the interference suffered by each user is also calculated. From this information, the value of the SINR experienced by each user for different frequency subbands is obtained. Once the main parameters of interest have been obtained, the functions of radio resource management are executed. At link level, the simulator includes link adaptation and resource scheduling functions.

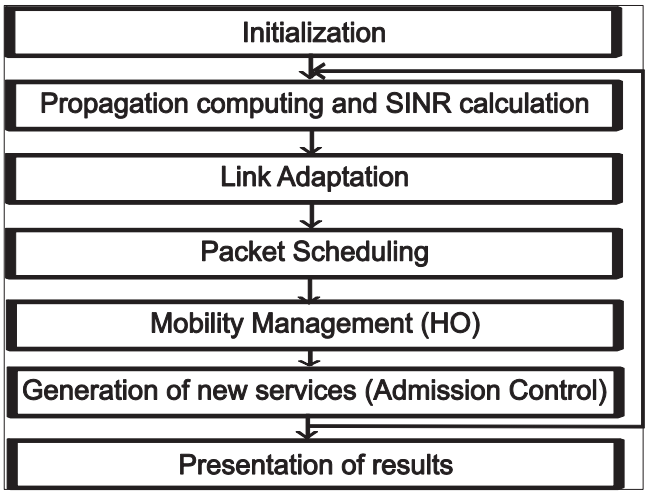

Fig. 1. Block diagram of the simulator.

The link adaptation function selects the most appropriate modulation and coding scheme for each user to transmit the information, maximizing spectral efficiency. This decision is based on the propagation conditions experienced by the user. The CQI indicator is used to represent the environment conditions. The radio resource scheduling function assigns available radio resources to users based on channel conditions experienced by each user for different frequency subbands. This function is also based on the CQI indicator.

At network level, the simulator includes several functions. The main ones are handovers and admission control. Lastly, the main results and statistics are shown.

A. Simulation Scenarios

In the simulator, two different scenarios have been developed: a macrocell scenario and a Manhattan scenario. The first one consists of a configurable number of hexagonal cells. In Manhattan, different types of elements such as buildings and roads are additionally defined and distributed along the cells of the scenario, shaping a rectangular grid.

Macrocell Scenario

This scenario models a macro-cellular environment. Fig. 2 illustrates the layout for a scenario with 19 tri-sectorized sites evenly distributed.

To avoid border effects in the simulation, the simulator incorporates the wrap-around technique described in [9]. Wrap-around consists in creating replicas of the scenario surrounding the original one. Only the original scenario is considered when collecting results and statistics. Fig. 3 shows the simulation scenario with the wrap-around technique.

Finally, it is necessary to define the set of interfering cells for each cell of the scenario. For each cell, an ordered set of interfering cells are constructed in terms of power received from each interferer by static system-level simulations.

Manhattan Scenario

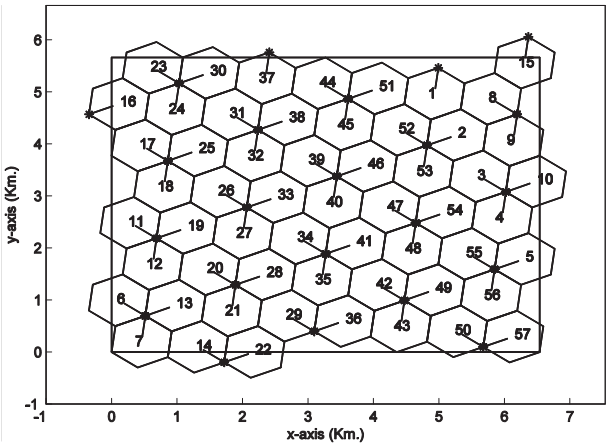

Fig. 2. Simulation scenario.

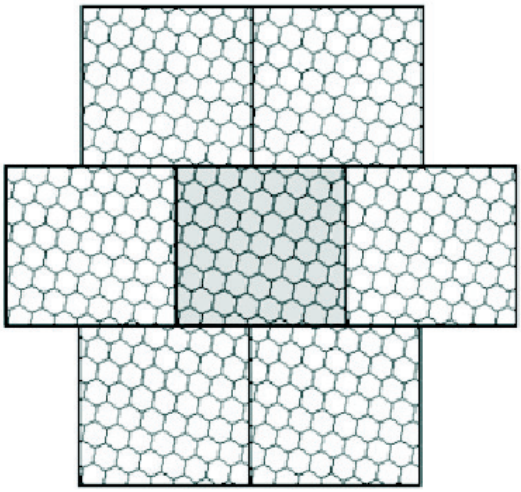

Fig. 3. Simulation scenario with wrap-around.

In this scenario, a set of buildings and roads are additionally defined. This scenario also includes the wrap-around technique. When defining the roads and the buildings, it is necessary to ensure that a user that leaves the original scenario, continues in a permitted area (e.g., a vehicle is not allowed to enter in the replica on a sidewalk or a block) in the replica scenario. Fig. 4 shows the case in which the wrap-around technique does not consider the difference between blocks and sidewalks in the definition of the scenario.

B. Spatial Traffic Distribution

Users can be spatially distributed in both an uniform or non-uniform way over the scenario. In the case of uniform spatial distribution, users are located in whatever point of the scenario with the same probability. However, to reproduce a realistic situation, it is recommended to use a non-uniform distribution. The typical spatial distribution in urban areas can be described by a lognormal distribution at a cell level. A function of traffic estimation is created adding to the log-normal distribution a Gaussian random variable [10]. Fig. 5 shows the probability of starting a call in any location of the scenario. It is observed that the spatial traffic distribution has a central peak, creating

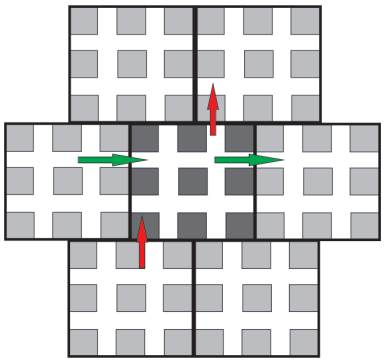

Fig. 4. Wrong design of the Manhattan scenario with wrap-around.

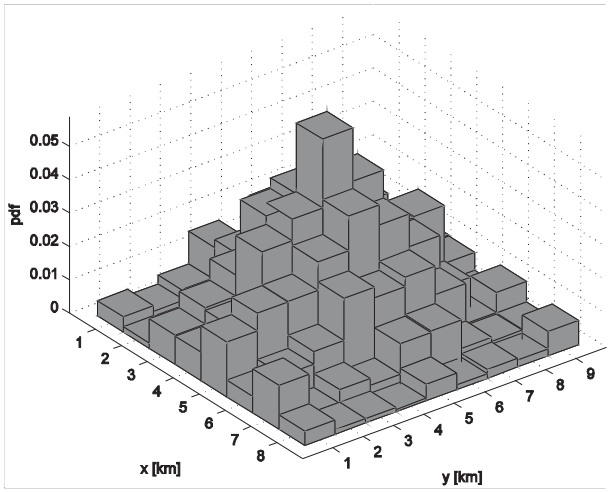

Fig. 5. Spatial traffic distribution.

a congested area with higher traffic density. It is noted that the spatial traffic distribution will be slightly affected by the mobility model, explained in the next section.

C. Mobility Model

The simulator includes two user mobility models. Regarding the user movement directions, a first model does not define any constraint about user directions. User can freely move over the scenario. The second model distinguishes between buildings and roads at the time of moving users along the scenario.

The first mobility model considers random constant paths for the users in the simulation scenario. Users move at constant speed, set to 3, 50 or 120 km/h. This model also includes the effect of the wrap-around technique, which means that when a user reaches the limit of the original scenario, appears in the correct position of this scenario, as shown in Fig. 6.

The second mobility model developed in the simulator emulates the realistic behavior of users in an urban environment. This model implements the behavior of different types of users in the urban environment: vehicles, buses, pedestrians and indoor users. Manhattan Mobility Model is used for outdoor users and Random Waypoint Model for indoor users [11]. The dimensions of buildings, streets and sidewalks are taken from a real urban environment (the 'Ensanche' area in Barcelona, Spain). Such values of elements are defined in Table I.

TABLE I
DIMENSION OF ELEMENTS IN A REAL SCENARIO

Block size	Street width	Road width	Sidewalks width
120 × 120 m	20 m	10 m	10 m

Manhattan Mobility model is implemented to describe the outdoor users (vehicles, buses, pedestrians) movement. This model is widely used to describe the movement of mobiles in urban areas by means of a grid road topology, as shown in Fig. 7. Users move along the streets and can turn at crosses with a given probability, that is recommended to be 25% probability to turn right and the same for a left turn [12]. In vehicles turn it is ensured that they are at the correct lane of the road for their new direction. The scenario is composed of vertical and horizontal streets perpendicular to each other. Every street has two lanes (each for one movement direction): North/South for vertical streets and East/West for horizontal streets. Vehicles move along a particular area of the street (road) and pedestrians move along another area (sidewalks). Buses behavior in the model is the same as those of vehicles, but providing the possibility to allocate multiple users sharing the same position, movement direction and speed. Studies on "moving hotspot" can be made with this type of users [13].

Additional features are included in the above-described Manhattan model to give more realism to the model. One of the features is the implementation of traffic lights at the street corners. Every street at an intersection has a traffic light [14]. Thus, the behavior of the network under conditions of user agglomeration in the corner where vehicles are stopped can be studied. To complete the Manhattan model for outdoor users, the wrap-around technique is implemented to avoid the border effects [9].

Indoor users follow a Random Waypoint mobility model [15]. Random Waypoint is a simple but very useful model to simulate users in buildings. The goal of implementing these users is to create some traffic load in specific cells. These users are modeled as static load, i.e. they do not leave the building in which they were created.

D. Traffic Model

Two types of service are considered: Voice over IP (VoIP) service and Best Effort (BE) service (similar to Full Buffer).

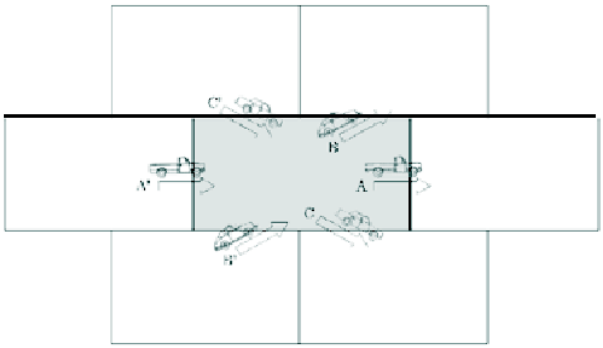

Fig. 6. First mobility model: random constant paths with wrap-around.

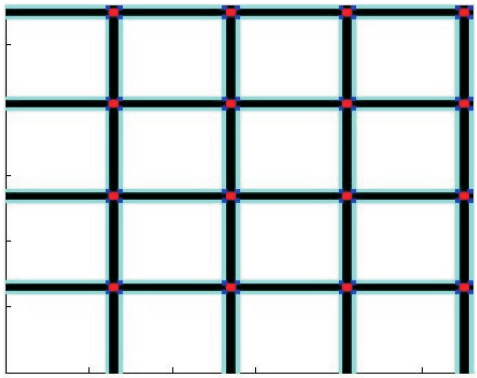

Fig. 7. Movement of outdoor users in a Manhattan scenario.

The VoIP service is defined as a source generating packets of 40 bytes every 20 ms [16], reaching a bit rate of 16 kbps. As it will be seen later, the radio resource allocation in the simulator is performed for time intervals of 10ms. For this reason, the voice service has been implemented as users that transmit packets of 20 bytes every 10 ms. For this service, it is necessary to determine when a call is dropped, that is, when the service is interrupted. Such an event occurs when a user does not receive packets during a specific time interval. For instance, user packets are not scheduled when the connection quality is below a certain threshold or there are not enough resources, so the call may be dropped.

The BE service is similar to the Full Buffer service. The Full Buffer service is defined as a user that has infinite data to transmit. For this reason, a Full Buffer user will always transmit with the maximum available bit rate if radio resources are assigned to him. This BE service allows to assess network performance in terms of throughput. The service implemented in the simulator maintains these features with the only difference that the user is active only during a period of time, that is, the service starts at a certain time of simulation and ends some time later. During that activity time, the user has unlimited information to transmit. Once the service is finished, both the time that the user has been active and the experienced bit rate are known so that it is possible to calculate the size of the packet received by the user.

III. PHYSICAL LAYER

A. Channel Model

The mobile radio channel can be described as a time-varying linear filter [17]. Therefore, it can be represented in the time domain by its impulse response, $h(\tau, t)$, where τ stands for delay of each path in h, and the amplitude of each path varies with time t.

Also, the channel can be characterized by the time-variant transfer function, $H(f, t)$, which is related with impulse response through the Fourier transform with respect to the delay variable τ.

When the behavior of the channel is randomly time variant, the above-mentioned channel functions become stochastic processes. A realistic approach to the statistical characterization

of such a channel may be accomplished in terms of correlation of channel functions since it enables channel output autocorrelation to be determined. Channel autocorrelation functions are related through Fourier transform as well.

For typical physical channels, time fading statistics can be assumed stationary over short periods of time and channel correlation function is invariant under a translation in time t, thus being categorised as wide-sense stationary (WSS). In addition, frequency-selective behaviour is stationary in frequency f being the autocorrelation function invariant under frequency translations. This condition is termed uncorrelated scattering (US), and most practical channels satisfy it fairly well.

Autocorrelation functions of wide-sense stationary uncorrelated scattering (WSSUS) channels exhibit the property that the time-variant transfer function autocorrelation is stationary both in time t and frequency f variables, i.e. its value does not depend on the absolute time or frequency considered but only on the time or frequency shift between time or frequency points of observation.

As a consequence, a WSSUS channel can be simulated generating the impulse response, $h(\tau, t)$, with stationary variation in time t for each path and no cross-correlation between different values of delay τ (i.e. generating independent stochastic processes for different paths). Stationarity is achieved by applying Doppler filters to the amplitude time t variation on each path. These filters perform spectrum shaping according to Doppler effect experimented by any radio signal propagating from a transmitter to a moving receiver (or vice versa). Afterwards, the frequency transfer function, $H(f, t)$, can be computed easily by applying the Fourier transform to the impulse response with respect to delay variable.

To simulate non-constant speed mobiles, fading realizations cannot be performed over time as an independent variable. Alternatively, space variables have to be used so that channel varies according to the current position of the mobile at each iteration of simulation.

Therefore, a fading channel spatial grid has been generated. This grid provides channel responses for every physical position in the simulated scenario, regardless of mobiles speed. In fact, mobiles can stay at a static position for a time interval, and then can start moving at any speed. This allows simulation of urban mobility pattern, where vehicle mobiles stop and afterwards go on because of traffic lights, or pedestrian users wandering inside a shopping centre.

Narrow band fading grid is generated to get a Lord Rayleigh universe [19]. In other words, following Clarke's model [17], a spatial bidimensional complex Gaussian variable is filtered by a bidimensional Doppler filter. The bandwidth of 2-D Doppler filter can be obtained as a function of spatial grid resolution and wavelength size.

Once narrowband channel behavior for each spatial position is obtained, extension to wideband is possible performing the same procedure for every path in power delay profiles described in the specification for Extended Typical Urban (ETU), Extended Pedestrian A (EPA) and Extended Vehicular A (EVA) channels in [18]. Thus, different (uncorrelated) Rayleigh universes are generated for each delay in wideband channel scenario. This results in a distance-variant impulse response $h(\tau, d)$ (autocorrelation) of the channel instead of a time-variant impulse response $h(\tau, t)$ described in [17] as one of the four system functions for complete WSSUS (Wide Sense Stationary Uncorrelated Scattering) channel characterization. The only difference is the time to distance (t to d) variable change made. A realization of the function is shown in Fig. 8.

Since the simulator requires channel realizations for different frequency bands (corresponding to OFDM subcarriers), the distance-variant impulse response has to be transformed into a distance-variant transfer function $H(f, d)$ at each position, by applying Fourier transform with respect to delay variable τ. An example of this function can be seen in Fig. 9.

The only remaining step is to extend the space variable d of the generated function $H(f, d)$ to a bidimensional (x, y) space variable, obtaining $H(f, x, y)$, a tridimensional function that

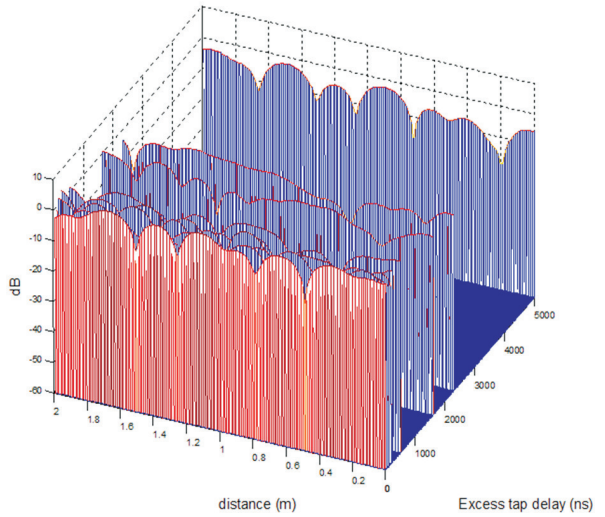

Fig. 8. Generated bidimensional channel impulse response for ETU channel model in [18].

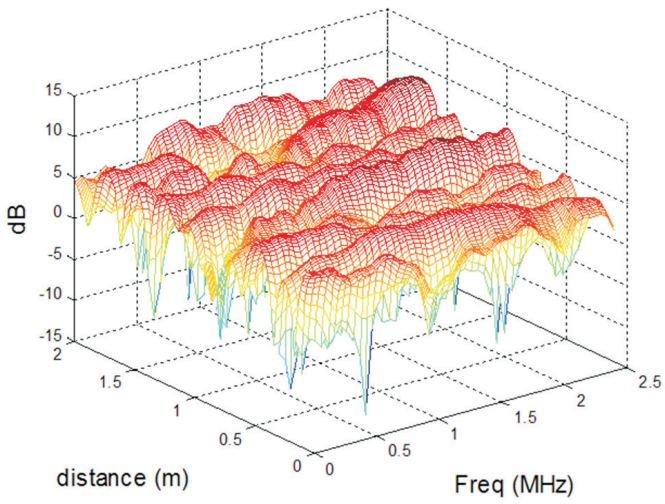

Fig. 9. Generated distance-variant transfer function for ETU channel model in [18].

provides frequency response for each spatial position given by coordinates, x and y.

B. Radio Propagation Channel

The simulator includes two alternatives for obtaining propagation calculations. As a first option, the calculations are performed at each iteration and whenever necessary (e.g., in the function that evaluates the channel conditions of each link or in the admission control function). Alternatively, propagation calculations are made from a set of pre-computed matrices. In this case, it is not necessary to perform the calculations during the simulation.

For the definition of the pre-computed propagation matrix, the scenario is divided into a grid, whose resolution is given by the correlation distance of the slow fading (20 m). To know the values of the propagation loss a user is experiencing, it is only necessary to read the position of the matrix corresponding to the position occupied by the user in the scenario relative to every base station and then interpolate it with other values of the matrix depending on the relative position in the grid. The propagation matrices include the path loss calculations and the slow fading.

In both options, the radio propagation model is the COST 231 extension of Okumura-Hata model [20]. This model is applicable for frequencies in the range from 1500 to 2000 MHz. The effective height of the base station or evolved-Node B (eNB) antenna has been set to 30 meters, while the effective height of the user equipment (UE) antenna has been set to 1.5 meters. With these assumptions and setting the operating frequency to 2 GHz, the expression for the propagation loss as a function of the distance is given by:

$$L = 134.79 + 35.22 \log d, \tag{1}$$

where d represents the distance in km between the UE and the eNB which the user is connected to.

In addition to the propagation loss, the simulator includes a slow fading model based on the fact that the local average of the radio signal envelope can be modeled by a lognormal distribution, i.e., the local average, in dB, is a Gaussian random variable. The standard deviation of the distribution depends on the considered environment. A typical value for the macrocell urban area analyzed is 8 dB [21].

For the choice of the propagation matrices, the value of shadowing is included in these matrices. The other alternative requires some additional calculations. The dynamic nature of the simulator leads to the implementation of a correlation model between the successive samples which represent the slow fading. An ARMA(1,1) model [22] has been selected for the simulator in this work,

$$z_t = \theta z_{t-1} + (1-\theta) a_t, \tag{2}$$

where z_t represents the slow fading sample at the current simulation step, z_{t-1} is the slow fading sample at the previous simulation step, a_t is a Gaussian random variable uncorrelated with z_t and θ and $(1-\theta)$ are the coefficients of the ARMA(1,1) model.

The coefficients of this model are determined from the probability that a user terminal suffers fading caused by the same obstacle at the time interval Δ/v. That probability can be modeled as an exponential distribution:

$$\theta = P(\tau < \Delta/v) = \exp(-\Delta \cdot \lambda) \tag{3}$$

where Δ is the distance moved by the user terminal at a time interval, v is the UE velocity and λ is the interruption rate of the line of sight. The interruption rate of the line of sight, λ, is the inverse of the correlation distance. A typical value of the correlation distance for the macrocell urban area simulated is 20 m (or 50m) [23].

Finally, the Gaussian random variable, a_t, must be defined based on its mean and standard deviation. This variable provides a statistical distribution of zero mean and a standard deviation, σ_a, that relates to the standard deviation of the slow fading, σ_z, as follows:

$$\sigma_z^2 = \frac{\sinh(\Delta \cdot \lambda/2)}{\cosh(\Delta \cdot \lambda/2)} \cdot \sigma_a^2 \tag{4}$$

Once the propagation calculations have been carried out, it is possible to study the link quality experienced by each user in terms of Signal to Interference Ratio (SIR). The next section describes the process to calculate the value of SIR for each user.

IV. Link Layer

A. SIR Calculation

The SIR is a representative measurement of the link quality that the user is experiencing. To calculate the SIR in the simulator, it is first necessary to calculate the interference experienced by each user. It is assumed that intracell interference is negligible in LTE because the scheduler assigns different frequencies and time slots to each user. Thus, only co-channel intercell interference due to the interfering cells using the same subcarriers is considered. This requires knowing the signal arriving to each user from all interfering cells. To calculate the interference from each base station to the terminal, the channel response is not taken into account, but only the path loss and slow fading are considered here.

The SIR calculation for a given subcarrier k, γ_k, is computed using the expression proposed in [24],

$$\gamma_k = P(k) \times \overline{G} \times \left(\frac{N}{N+N_p}\right) \times \frac{R_D}{N_{SD}/N_{ST}}, \tag{5}$$

where $P(k)$ represents the frequency-selective fading power profile value for the k^{th} subcarrier, $\overline{G}$ includes the propagation loss, the slow fading, the thermal noise and the experienced interference, N is the FFT size used in the OFDM signal generation, N_p is the length of the cyclic prefix, R_D indicates the percentage of maximum total available transmission power allocated to the data subcarriers, N_{SD} is the number of data subcarriers per Transmission Time Interval (TTI) and N_{ST} is the number of total useful subcarriers per TTI.

If it is assumed that the multipath fading magnitudes and phases are constant over the observation interval, the frequency selective fading power profile value for the k^{th} subcarrier can be calculated using the expression

$$P(k) = \left| \sum_{p=1}^{paths} M_p A_p \exp(j[\theta_p - 2\pi f_k T_p]) \right|^2, \tag{6}$$

where p is the multipath index, M_p and θ_p represent the amplitude and the phase values of the multipath fading respectively, A_p is the amplitude value corresponding to the long-term average power for the p^{th} path, f_k is the relative frequency offset of the k_{th} subcarrier within the spectrum, and T_p is the relative time delay of the p^{th} path. In addition, the fading profile is assumed to be normalized such that $E[P(k)] = 1$.

The value of $\overline{G}$ is calculated from the expression:

$$\overline{G} = \frac{P_{max} \dfrac{g_n(UE) \times g_{UE}}{PL_{UE,n} \times SH_{UE,n}}}{P_{noise} + \displaystyle\sum_{k=1, k\neq n}^{N} P_{max} \times \frac{g_k(UE) \times g_{UE}}{PL_{UE,k} \times SH_{UE,k}}}, \quad (7)$$

where $g_n(UE)$ is the antenna gain of the serving base station in the direction of the user UE, g_{UE} is the antenna gain of the user terminal, P_{noise} is the thermal noise power, $PL_{UE,k}$ is the propagation loss between the user and the eNB k, $SH_{UE,k}$ is the loss due to slow fading between the user and the eNB k and N is the number of interfering eNBs considered (set to 43 in the simulator).

A Physical Resource Block (PRB) is the minimum amount of resources that can be scheduled for transmission in LTE. As a PRB comprises 12 subcarriers, it is necessary to translate those SIR values previously calculated for each subcarrier into a single scalar value. This can be made using the Exponential Effective SINR Mapping, which is based on computing the effective SIR by the equation

$$SIR_{eff} = -\beta \ln \left(\frac{1}{N_u} \sum_{k=1}^{N_u} \exp\Big(-\frac{\gamma_k}{\beta} \Big) \right), \quad (8)$$

where β is a parameter that depends on the Modulation and Coding Scheme (MCS) used in the PRB [25] assuming that all subcarriers of the PRB have the same modulation and N_u indicates the number of subcarriers used to evaluate the effective SIR. The values of β have been chosen so that the block error probability for all the subcarriers are similar to those obtained for the effective SIR in a AWGN channel [26]. The value of β for a particular MCS is shown in Table II.

Once the effective SIR has been calculated, the Block Error Rate (BLER) showing the connection quality can be derived. There exist curves that establish the relationship between the values of SIR and BLER defined for an AWGN channel for every modulation and coding rate combination. These curves can also be used to calculate the BLER because intercell interference is equivalent to AWGN as the value of β has been selected for this purpose.

B. Hybrid Automatic Repeat Request Scheme

The Hybrid Automatic Repeat reQuest (H-ARQ) is a function at link level that allows to perform retransmissions directly at physical or MAC layer in LTE. A low-complexity model capable of accurately predicting the H-ARQ gains on the physical layer is derived in [27]. When an H-ARQ retransmission occurs, an improvement of the BLER is expected. The result is that the BLER curves based on AWGN channel model are shifted providing a Signal to Noise Ratio (SNR) gain due to H-ARQ. Hence, the new SIR can be calculated as follows:

$$SIR(i) = SIR + SRN_{gain}(i), \quad (9)$$

where i represents the i^{th} retransmission. The value of SNR_{gain}, which depends on the redundancy version index i and the given MCS can be derived from a specific table given in [27].

Once the value of BLER has been obtained and taking into account the MCS used in the transmission, it is possible to calculate the value of throughput, T_i, for each user as follows:

$$T_i = (1 - BLER(SIR_i)) \times \frac{D_i}{TTI}, \quad (10)$$

where D_i is the data block payload in bits [28], which depends on the MCS selected for the user in that time interval, TTI is the transmission time interval and $BLER(SIR_i)$ is the value of BLER obtained from the effective SIR.

TABLE II
VALUES OF B DEPENDING ON THE MODULATION AND CODING SCHEME

Modulation	Coding	β factor	Modulation	Coding	β factor
QPSK	1/3	1.49	16QAM	3/4	7.33
QPSK	2/5	1.53	16QAM	4/5	7.68
QPSK	1/2	1.57	64QAM	1/3	9.21
QPSK	3/5	1.61	64QAM	2/5	10.81
QPSK	2/3	1.69	64QAM	1/2	13.76
QPSK	3/4	1.69	64QAM	3/5	17.52
QPSK	4/5	1.65	64QAM	2/3	20.57
16QAM	1/3	3.36	64QAM	17/24	22.75
16QAM	1/2	4.56	64QAM	3/4	25.16
16QAM	2/3	6.42	64QAM	4/5	28.38

C. Link Adaptation

Before explaining the Link Adaptation function, the 3GPP standardized parameter known as Channel Quality Indicator (CQI) is described. Such an indicator represents the connection quality in a subband of the spectrum. The resolution of the CQI is 4 bits, although a differential CQI value can be transmitted to reduce the CQI signaling overhead. Thus, there is only a subset of possible MCS corresponding to a CQI value [29]. QPSK, 16QAM and 64QAM modulations may be used in the transmission scheme. In the simulator, the CQI is reported by the user to the base station each iteration (100 ms).

Based on CQI values, the link adaptation module selects the most appropriate modulation and coding scheme to transmit the information on the physical downlink shared channel (PDSCH) depending on the propagation conditions of the environment. To quantify the link quality for each user and for each subband of the spectrum, the CQI index is used to provide this information. If the experienced BLER value is required to be smaller than a specific value given by the service, it is possible to establish a SIR-to-CQI mapping that allows to select the most appropriate MCS from a given value of SIR [8]. The standard 3GPP defines a 5-bit modulation and coding scheme field of the downlink control information to identify a particular MCS. This leads to a greater variety of possible modulation and coding schemes. For simplicity, the developed LTE simulator includes only the same set of MCS given by the CQI index. From the effective SIR value, the index CQI is

calculated and the MCS can be determined for the next time interval.

D. Resource Scheduling

The Resource Scheduling can be decomposed into a time-domain and frequency-domain scheduling. On the one hand, it is necessary to determine which user transmits at the following time interval. On the other hand, the frequency-domain scheduler selects those subcarriers within the system bandwidth whose channel response is more suitable for the user transmission. For this purpose, the channel response for each user and for each subcarrier of the system bandwidth has to be estimated. Such a piece of information is given by the channel realizations generated in the initialization phase of the simulation, assuming a perfect estimation of the channel response. To select the most appropriate frequency subband for the user, the CQI index is used.

The developed simulator includes different strategies for radio resource scheduling. In all of them, the CQI parameter gives the information of the channel quality experienced by each user. Likewise, scheduling is done for each cell at each iteration following the configured strategy [30]. The following paragraphs describe the scheduling algorithms implemented in the simulator.

Best Channel Scheduler (BC)

In this scheduler, both time-domain and frequency-domain scheduling are done for a more efficient use of resources. At each iteration, all users are sorted based on the quality experienced for each PRB, which is obtained from CQI values. Once the users are sorted, the allocation will proceed until there are not available radio resources or no more users to transmit.

The resource allocation is made following the expression:

$$\hat{\imath}[n] = \arg\max_{i}\{r_{ik}[n]\}, \tag{11}$$

where $\hat{\imath}$ is the selected user i, and r_{ik} is the estimated achievable throughput for PRB k and user i obtained from the CQI.

This scheduling algorithm maximizes the overall system efficiency because the resource allocation is done looking for the combinations PRB-user with better channel conditions. The disadvantage of this algorithm is that harms users with bad channel conditions. Thus, if a user is far from the serving eNB or has a deep fading for prolonged periods of time, it cannot be scheduled and can suffer significant delays.

Round Robin to Best Channel Scheduler (RR-BC)

This scheduler uses different strategies for time-domain and frequency-domain scheduling. For time-domain scheduling, the Round Robin method is applied. Thus, users are selected cyclically without taking into account the channel conditions experienced by each of them. Then, each PRB is assigned to the user with a higher potential transmission rate for that PRB (transmission rate is estimated based on the user's CQI value for each PRB).

At each iteration and for each base station, the expressions to be evaluated are:

$$\hat{\imath}[n+1] = (\hat{\imath}[n]+1)\mathrm{mod}N_u, \tag{12}$$

$$\hat{k}[n] = \arg\max_{k}\{r_{ik}[n]\}, \tag{13}$$

where $\hat{\imath}$ is the selected user, N_u is the number of users and $\hat{k}$ represents the PRB selected. In this case, the goal is to maximize system efficiency, but trying not to harm users with unfavorable channel conditions.

Large Delay First to Best Channel Scheduler (LDF-BC)

This scheduler is similar to the previous one only differing in time-domain scheduling. In this case, instead of cyclically selecting the users, they are sorted by the time they have spent without transmitting. Thus, if for some reason, such as a fading prolonged in time, the user has not been allocated in previous iterations, he will get a higher priority in the current iteration.

In the same way as in the previous case, at each iteration and for each base station the allocation is carried out based on the following terms:

$$\hat{\imath}[n] = \arg\max_{i}\{W_i[n]\}, \tag{14}$$

$$\hat{k}[n] = \arg\max_{k}\{r_{ik}[n]\}, \tag{15}$$

where $W_i[n]$ is the number of iterations without transmitting for user i. At the end of each iteration, the value of $W_i[n]$ is updated for all the users based on whether they have been allocated or not.

Proportional Fair (PF)

The Proportional Fair scheduler is an algorithm similar to Best Channel, but it tries not to harm users with worse channel conditions. The objective of this algorithm is to find a balance between getting the maximum possible efficiency of the channel and keeping fairness between users. To this end, scheduling is not only based on the potential transmission rate but also takes into account the average transmission rate of the user in previous iterations. The algorithm follows the expression:

$$\hat{\imath}[n] = \arg\max_{i}\left\{\frac{r_{ik}[n]}{\overline{r}_i}\right\}, \tag{16}$$

where r_i is the average transmission rate experienced by user i.

Scheduler for Different Types of Service

As mentioned before, the simulator includes two different types of service, i.e., voice service and best effort service. To schedule all users, a division between the two types of service is made. The scheduler strategy can be different for each service. Also, the radio resources are divided into two groups. One of them is reserved for voice users who need to meet a constant bit rate and the other group can be used for best effort users that can maximize their throughput based on channel conditions. The division of the PRB in these two groups is configurable.

V. Network Layer

The success of cellular networks is based on the fact that users can obtain global support while moving (coverage, access...). While physical and link level define the propagation and transmission characteristics along the UE-eNB link, network level manages all base stations, terminals and their resources as a whole.

The main network level functionalities rely on Radio Resource Management (RRM) processes. This section describes the Admission Control (AC), Congestion Control (CC) and HandOver (HO) techniques implemented in the simulation tool. It should be pointed out that, although scheduling is also usually labeled as an RRM technique, it has been already described in previous sections since it is located at link level in the simulation tool.

A. Admission Control

Once an UE decides to start a connection, a first decision is which cell will serve that connection. Such a decision is taken through two main steps:

1) *Minimum Reference Signal Received Power* (RSRP). UE collects and sends to the network reference signal received levels from the serving cell and its neighbors. Cells are ordered from higher to lower levels and candidate cells are those fulfiling:

$$RSRP(i) \geq MinThresholdLEV(i), \qquad (17)$$

where $RSRP(i)$ is a wideband measurement meaning the received level for the reference signals in cell i, and $MinThresholdLEV$ is the minimum required signal level to be accepted. Minimum level is defined on a cell basis. Finally, the best 'i' cell in the list is initially selected.

2) *Enough free resources.* The availability of free PRBs in best cell is then checked. Note that the mobile network does not know how many PRBs will require the user data connection once it is admitted. Signal-level measurements are taken from the reference signals, but radio channel conditions could be quite different for the finally assigned data radio channel (e.g., fast fading, interference). That is the reason why a 'worst-case' criterion has been taken to accept UEs. Thus, the UE is finally accepted if:

$$freePRB(i) \geq MaxPRB(serv), \qquad (18)$$

where $freePRB(i)$ is the number of PRBs available in cell i, and $MaxPRB(serv)$ is the worst-case PRB requirement (i.e., the highest number of PRBs needed to maintain a connection) that a specific type of service, '$serv$', would demand along the entire connection.

If there are not enough free PRBs, the next candidate cell in the list is checked. A user connection is blocked when no cell fulfils (17) and (18).

B. Congestion Control

Congestion control avoids congestion situations in the network. This technique usually defines a pool of resources which will be assigned differently than by admission control.

Operators give priority to ongoing connections over fresh calls [31]. If both fresh and ongoing users are in conflict for the same radio resources (e.g., a handover and a fresh connection occur simultaneously), existing users should be first scheduled. With that aim, fresh users will not be accepted in a cell if:

$$LR(i) \geq LRthreshold, \qquad (19)$$

where $LR(i)$ is the Load Ratio in cell i, and $LRthreshold$ is the congestion threshold. There is a trade-off when selecting the $LRthreshold$ value. A too low value might cause call dropping from rejected incoming handovers, but a very high level could lead to unnecessary call blocking while protected resources are idle.

C. Handover

The HO algorithm is the main functionality to manage the connected user mobility. HO algorithms are vendor specific. The following paragraphs describe classical handover algorithms proposed for LTE and implemented in the simulator.

Quality Handover (QualHO)

A QualHO is triggered when:

$$RSRQ(i) \leq RSRQ_{threshold}(i) \qquad \text{for TTT}^{Qual} \text{ seconds}, \qquad (20)$$

and

$$RSRP(j) - RSRP(i) \geq Margin_{Qual}(i,j), \qquad (21)$$

where RSRQ is the Reference Signal Received Quality, usually measured by the Signal to Interference and Noise Ratio (SINR) for the references signals, RSRP is the Reference Signal Received Power, TTT^{Qual} is Time-To-Trigger value, and $Margin_{Qual}$ is the level hysteresis between server and adjacent cells (i and j, respectively).

This QualHO aims to re-allocate connections which are experiencing a bad quality connection to other cells. $Margin_{Qual}$ is defined on an adjacency basis.

For monitoring purposes, a QualHO is classified as an Interference HO (IntHO) if

$$RSRP(i) \geq RxLEV^{Interf}_{threshold}(i) \quad \text{for TTT}^{Qual} \text{ seconds}, \qquad (22)$$

i.e., the UE have a high signal level but low SINR figures.

Minimum Level Handover (LevHO)

A LevHO is triggered when:

$$RSRP(i) \geq MinRxLEV_{LevHO}(i), \qquad (23)$$

and

$$RSRP(j) - RSRP(i) \geq Margin_{Lev}(i,j), \qquad (24)$$

where $MinRxLEV_{LevHO}$ is a minimum signal level threshold. LevHO aims to re-allocate connections experiencing

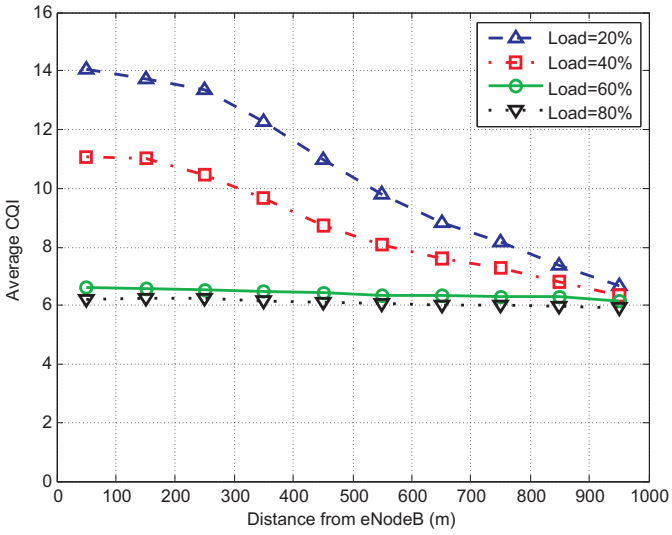

Fig. 10. Average CQI as a function of the distance for different traffic load levels.

a very low signal level (e.g., when the UE is getting out of coverage area). LevHO is considered an 'urgent' HO and must be triggered as soon as possible. Thus, no Time-to-Trigger parameter has been considered.

Power Budget Handover (PBGT_ HO)

A PBGT_HO is triggered when:

$$RSRP(j) - RSRP(i) \geq Margin_{PBGT}(i,j), \qquad (25)$$

In this case, there is no first condition to be fulfiled. Equation (25) is only evaluated every N^{PBGT} seconds. PBGT_HO is not considered an urgent HO, but an optimization algorithm. At the end of a PBGT_HO process, the UE should be connected to the best cell in terms of signal level (provided that $Margin_{PBGT}$ is positive).

VI. Evaluation of System Performance

In this section, several reference scenarios are simulated to evaluate system performance. These are termed 'reference' because network parameters (e.g., HO margin or load ratio threshold in the Admission Control) are set to a moderate default value. For voice service, system performance is evaluated by testing different levels of traffic demand and different strategies of scheduling. For best effort service, system performance is quantified in terms of cell throughput.

A. Key Performance Indicators

For voice service, a figure of merit widely used by network operators is the Call Dropping Ratio (CDR), defined as:

$$CDR = \frac{N_{dropped}}{N_{finished}} = \frac{N_{dropped}}{N_{dropped} + N_{succ}}, \qquad (26)$$

where $N_{dropped}$ is the number of dropped calls, N_{succ} is the number of successfully finished calls and $N_{finished}$ is the total number of finished calls. The simulation tool assumes that a call is dropped when a percentage of data packets are dropped during a specific time interval. Packet dropping may occur not only because there is no enough connection quality to be scheduled, but also because there are no available resources to be scheduled.

TABLE III
Simulation Parameters

Parameter	Configuration
Cellular layout	Hexagonal grid, 57 cells (3×19 sites), cell radius 0.5 km
Transmission direction	Downlink
Carrier frequency	2.0 GHz
System bandwidth	5 MHz
Frequency reuse	1
Propagation model	Okumura-Hata with wrap-around Log-normal slow fading, σ=8dB, correlation dist=20m Multipath fading, EPA model
Mobility model	Random direction, constant speed 3 km/h
Service model	VoIP: Poisson traffic arrival, mean call duration 120s, 16 kbps Best effort: full buffer, Transport Block size exact fit to PRB allocation
Base station model	Tri-sectorized antenna, SISO, EIRPmax=43dBm
Scheduler	Round Robin – Best Channel Large Delay First – Best Channel Resolution: 1 PRB
Power control	Equal transmit power per PRB
Link Adaptation	Fast, CQI based, Perfect estimation
RRM features	Directed Retry HO: QualHO, LevHO, IntHO, PBGT_HO
HO parameter settings	Time-To-Trigger = 100 ms HO margin = 3 dB
Traffic distribution	Log-normal distribution Unevenly distributed in space
Time resolution	Iteration time = 100 TTI (100 ms) Epoch time configurable

To quantify how efficiently resources are used, another performance indicator is the Call Blocking Ratio (CBR), which can be determined by the following expression:

$$DBR = \frac{N_{blocked}}{N_{offered}} = \frac{N_{blocked}}{N_{blocked} + N_{accepted}}, \qquad (27)$$

where $N_{blocked}$ and $N_{accepted}$ are the number of blocked and accepted calls by the admission control respectively, and $N_{offered}$ is the total number of offered calls.

Regarding BE traffic, cell throughput is a useful measure of spectral efficiency. The process to calculate this performance indicator was described in previous sections. Another indicator representing the link quality experienced by users is the CQI, which was also defined in previous sections.

To check the impact of traffic demand on network performance, several performance indicators are evaluated. To estimate the overall load level during the simulation, the average percentage of occupied PRBs in the system is monitored. This can be calculated as:

$$\rho = \frac{\sum_{k=1}^{N_{users}} N_k}{N_{total}}, \qquad (28)$$

where N_k is the current number of PRBs occupied by user k, N_{users} is the number of users and N_{total} is the total number of PRBs in the cell.

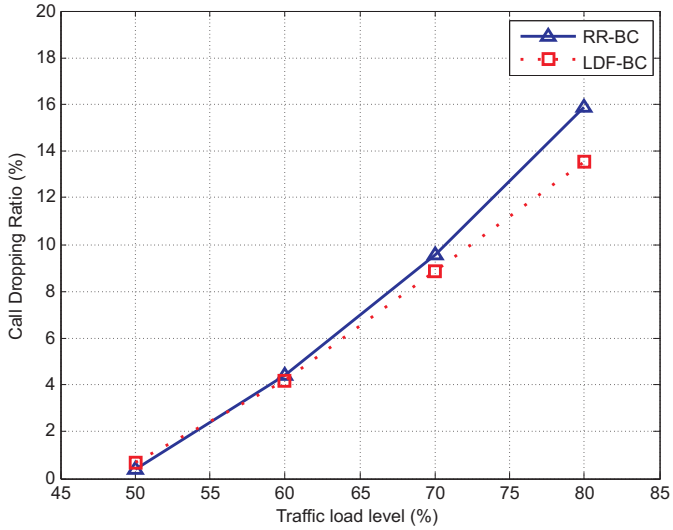

Fig. 11. Call Dropping Ratio as a function of the traffic load for two scheduling schemes.

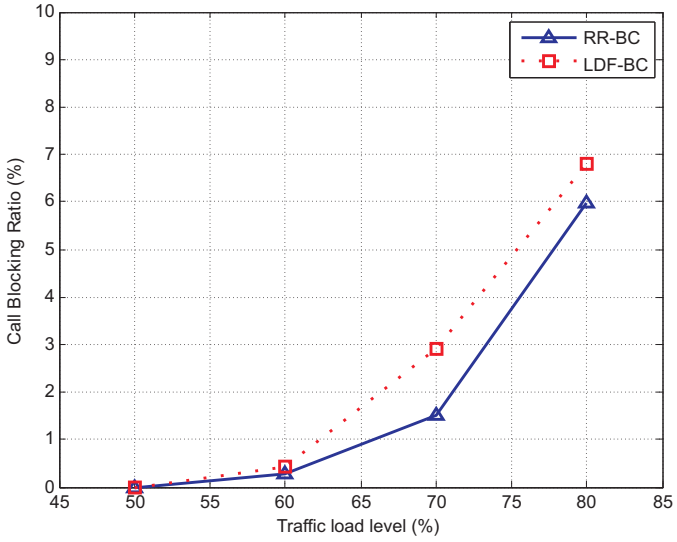

Fig. 12. Call Blocking Ratio as a function of the traffic load for two scheduling schemes.

B. Simulation Parameters

The simulated scenario includes a macro-cellular environment whose layout consists of 19 tri-sectorized sites evenly distributed in the scenario. The main simulation parameters for the simulations are summarized in Table III.

C. Performance Results

The first simulation is carried out to evaluate performance when only the voice service is offered by the network. In this case, measurements of CDR, CBR and CQI are collected for different levels of traffic load and different types of schedulers. Fig. 10 represents the dependency of the average CQI value on the distance for several load levels. As expected, the CQI value decreases as the distance from the base station is higher due to the path loss. Also it is noted that the range of variation of the CQI is much lower when the load level is higher. This is because the interference term in the expression of SIR becomes more important as the load level is increased, leading to a more restrictive set of CQI values in the cell coverage area.

Regarding call dropping, Fig. 11 shows the CDR for several levels of traffic load and two different scheduling schemes. The solid blue line represents the measured CDR when the scheduling strategy is RR-BC, while the dotted red line depicts the measured CDR when the scheduling strategy is LDF-BC. The difference between these two approaches is that LDF-BC sorts the users by the time they have spent without transmitting instead of cyclically sorting them according to the Round-Robin strategy. The LDF-BC scheme leads to a lower CDR for the same load level due to those users that get more priority in scheduling as they experience higher delay, avoiding call dropping.

The CBR for the two previous scheduling strategies as a function of the traffic load is illustrated in Fig. 12. As it is expected, the CBR increases as the traffic load level is higher. However, it is noted that the CBR is higher for the LDF-BC scheduling. This is because a lower CDR due to the scheduling strategy leads to a higher traffic load in the system, increasing the CBR. Logically, it is not appropriate to increase the network capacity by dropping ongoing calls. Thus, it can be concluded that the LDF-BC scheduler provides better performance than the RR-BC scheduler.

Another simulation has been carried out to quantify the network capacity. For this purpose, only the best effort service based on the full buffer traffic model is activated in the simulation tool. Thus, all PRBs are fully exploited and the cell throughput is a useful measurement to estimate the network capacity. The results are presented in Fig. 13 as the overall cumulative distribution function of cell throughput.

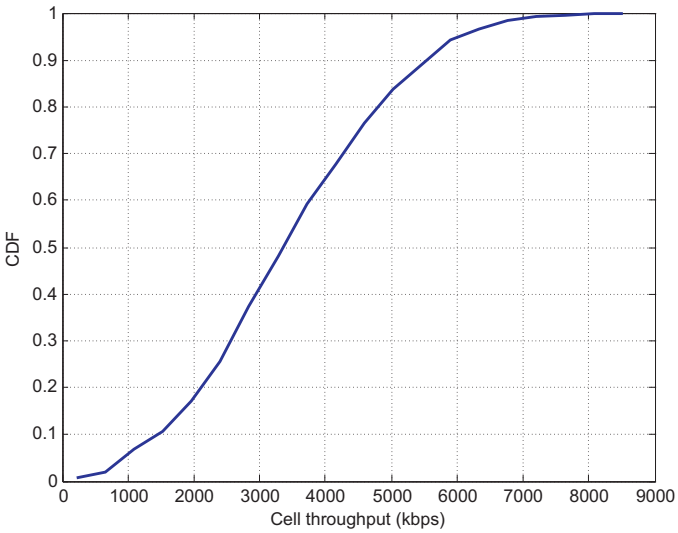

Fig. 13. Cumulative distribution function of downlink cell throughput.

VII. Conclusion

In this work, a computationally-efficient dynamic system-level LTE simulator has been described. This simulator includes the main characteristics of the radio access technology as well as the radio resource management algorithms which provide notable improvements in the efficient use of the available radio resources. For this purpose, the simulator has been implemented so that simulations require a low computational cost. A simulation is composed of epochs to evaluate the modification of network parameters performed by optimization algorithms.

At physical and link layers, this work focuses on the calculation of several indicators with the purpose of evaluating the connection quality in a mobile communication. Those indicators are required in the execution of radio resource management functions. Hence, it is essential that these indicators reflect accurately the behavior of a real network. To achieve this goal, an OFDM channel model has been performed to characterize the temporary and frequency variation of the radio transmission environment for each user during the simulation.

The main functions of radio resource management have been also described in this paper. At link level, the previous calculated indicators are inputs of the Link Adaptation and Dynamic Scheduling functions. At network level, the main functions are admission control and mobility management, whose parameters can be modified to evaluate optimization algorithms.

Finally, several simulations have been carried out. Results show network performance in terms of several indicators for different traffic load levels and scheduling schemes.

References

[1] 3GPP TS 36.201, "Evolved Universal Terrestrial Radio Access (E-UTRA); LTE physical layer; General description".

[2] 3GPP TS 36.300, "Evolved Universal Terrestrial Radio Access (E-UTRA) and Evolved Universal Terrestrial Radio Access Network (EUTRAN); Overall description".

[3] H. Holma and A. Toskala, *LTE for UMTS – OFDMA and SC-FDMA Based Radio Access*. Wiley, 2009.

[4] 3GPP TS36.133, "Evolved Universal Terrestrial Radio Access (E-UTRA); Requirements for Support of Radio Resource Management".

[5] J. Wu, Z. Yin, J. Zhang, and W. Heng, "Physical Layer Abstraction Algorithms Research for 802.11n and LTE Downlink," *International Symposium on Signals Systems and Electronics (ISSSE)*, 2010.

[6] J. Olmos, A. Serra, S. Ruiz, M. Garca-Lozano, and D. Gonzalez, "Link Level Simulator for LTE Downlink," *COST2100*, 2009, TD(09)779.

[7] J. C. Ikuno, M. Wrulich, and M. Rupp, "System Level Simulation of LTE Networks," *IEEE 71st Vehicular Technology Conference (VTC 2010-Spring)*, 2010.

[8] C. Mehlführer, M. Wrulich, J. C. Ikuno, D. Bosanska, and M. Rupp, "Simulating the Long Term Evolution Physical Layer," *17th European Signal Processing Conference (EUSIPCO 2009)*, 2009.

[9] T. Hytönen, *Optimal Wrap-around Network Simulation*. Helsinki University of Technology Institute of Mathematics: Research Reports, 2001.

[10] B. Ahn, H. Yoon, and J. W. Cho, "A Design of Macro-micro CDMA Cellular Overlays in the Existing Big Urban Areas," *IEEE Proceedings of Vehicular Technology Conference (VTC 2001)*, pp. 2094–2104, 2001.

[11] I. Khider, A. Saad, and W. Furong, "Study on Indoor and Outdoor Environment for Mobile Ad Hoc Network Supported with Base Stations," *Wireless Communications, Networking and Mobile Computing (WiCom)*, 2007.

[12] ETSI TR 101 112 v.3.2.0, Selection procedures for the choice of radio transmission technologies of the UMTS (UMTS 30.03 version 3.1.0), ETSI April 1998.

[13] A. Lobinger, S. Stefanski, and T. Jansen, "Load Balancing in Downlink LTE Self-Optimizing Networks," *IEEE 71st Vehicular Technology Conference, (VTC 2010-Spring)*, 2010.

[14] A. Mahajan et al, "Urban Mobility Models for VANETs," *2nd Workshop on Next Generation Wireless Networks*, 2006.

[15] T. Camp, J. Boleng, and V. Davies, "A Survey of Mobility Model for Ad Hoc Network Research," *Wireless Communication and Mobile Computing (WCMC): Special Issue on Mobile AdHoc Networking: Research, Trends and Applications*, vol. 2, no. 5, pp. 483–502, 2002.

[16] NGMN, "NGMN Radio Access Performance Evaluation Methodology", Version 1.0, Enero 2008, www.ngmn.org.

[17] J. D. Parsons, *The Mobile Radio Propagation Channel*. Pentech, 1992.

[18] 3GPP, "Evolved Universal Terrestrial Radio Access (E-UTRA); User Equipment (UE) Radio Transmission and Reception (Release 9)", 3GPP TS 36.101, Dec. 2009.

[19] W. C. Jakes, *Microwave Mobile Communications*. Wiley, 1974.

[20] E. Bonek, "Tunnels, Corridors, and Other Special Environments," in *COST Action 231: Digital Mobile Radio Towards Future Generation Systems*, C. E. Damosso, Ed. Brüssel: European Union Publications, 1999, pp. 190–207.

[21] F. Khan, *LTE for 4G Mobile Broadband: Air Interface Technologies and Performance*. New York, NY, USA: Cambridge University Press, 2009.

[22] D. Huo, "Simulating Slow Fading by Means of One Dimensional Stochastical Process," *IEEE 46th Vehicular Technology Conference, 1996. 'Mobile Technology for the Human Race'*, vol. 2, pp. 620–622, April-May 1996.

[23] M. Gudmundson, "Correlation Model for Shadow Fading in Mobile Radio Systems," *Electronics Letters*, vol. 27, no. 23, pp. 2145–2146, November 1991.

[24] 3GPP, "Feasibility study for Orthogonal Frequency Division Multiplexing (OFDM) for UTRAN enhancement", 3GPP TR 25.892, 2004.

[25] 3GPP, "System Analysis of the Impact of CQI Reporting Period in DL SIMO OFDMA (R1-061506)", Shanghai, China, 3GPP TSG-RAN WG1 45, May 2006.

[26] E. Tuomaala, "Effective SINR Approach of Link to System Mapping in OFDM/Multi-Carrier Mobile Network," *IEEE Mobility Conference, The Second International Conference on Mobile Technology Applications and Systems*, 2005.

[27] J. C. Ikuno, M. Wrulich, and M. Rupp, "Performance and Modeling of LTE H-ARQ," *International ITG Workshop on Smart Antennas WSA*, 2009.

[28] 3GPP, "OFDM-HSDPA System level simulator calibration (R1-040500)", Montreal, Canada, 3GPP TSG-RAN WG1 37, May 2004.

[29] 3GPP, "E-UTRA; UE conformance specification; Radio transmission and reception; Part 1: Conformance testing", 3GPP TS 36.521, 2009.

[30] J. T. Entrambasaguas, M. C. Aguayo-Torres, G. Gomez, and J. F. Paris, "Multiuser Capacity and Fairness Evaluation of Channel/QoS-Aware Multiplexing Algorithms," *IEEE Network*, vol. 21, no. 3, May-June 2007.

[31] D. Hong and S. S. Rappaport, "Traffic Model and Performance Analysis for Cellular Mobile Radio Telephone Systems with Prioritized and Nonprioritized Handoff Procedures," *IEEE Transactions on Vehicular Technology*, vol. 35, no. 3, pp. 77–92, 1986.